Sensitivity of vocal fold vibratory modes to their three-layer structure: Implications for computational modeling of phonation

Q. Xue and X. Zheng
Department of Mechanical Engineering, Johns Hopkins University, 126 Latrobe Hall, 3400 North Charles Street, Baltimore, Maryland 21218

S. Bielamowicz
Division of Otolaryngology, The George Washington University, Washington, DC. 20052

R. Mittal[a)]
Department of Mechanical Engineering, Johns Hopkins University, 126 Latrobe Hall, 3400 North Charles Street, Baltimore, Maryland 21218

(Received 2 December 2010; revised 23 March 2011; accepted 22 May 2011)

The sensitivity of the eigenmodes and eigenfrequencies of the human vocal fold to its three-layer structure is studied using finite-element modeling. The study covers a variety of three-dimensional vocal fold models ranging from an idealized, longitudinally uniform structure to a physiologically more realistic, longitudinally varying structure. Geometric parameters including the thickness of the ligament and cover layers as well as the ligament length are varied systematically. The results indicate that vocal fold vibratory modes are quite insensitive to the longitudinal variation in the thickness of the three layers as well as the variation in ligament length. However, significant overall changes in thickness of each layer can produce noticeable changes in these modes. The implications of these findings on computational modeling of phonation are discussed. © *2011 Acoustical Society of America*.
[DOI: 10.1121/1.3605529]

PACS number(s): 43.70.Bk [DAB] Pages: 965–976

I. INTRODUCTION

The wide range of phonation frequencies and complex vibratory characteristics in humans is believed to result from the relatively complex multi-layered structure and the material properties of vocal folds (Hirano, 1977; Alipour and Titze, 1991). From a histological viewpoint, the structure of the vocal folds can be separated into five different tissue layers: the epithelium, basal lamina, superficial layer of the lamina propria, deep layer of the lamina propria, and the thyroaryenoid muscle (or vocalis) (Titze, 1994). Mathematical modeling of vocal fold vibration usually requires the modeling of this inner structure; however, while there is some general understanding of the topology of this internal structure from a few carefully performed histological studies (Hirano, 1977; Hirano *et al.*, 1981), this internal structure likely varies from individual to individual depending on factors such as gender, race, age, and health. The extent of this variance is not well understood and this is likely due to the fact that current imaging techniques neither have the resolution nor the sensitivity to resolve this internal structure.

While the uncertainty inherent in the internal topology of the vocal folds has neither inhibited the development nor the successful use of mathematical models for gaining insights into the biophysics of phonation (Berry *et al.*, 1996; Alipour *et al.*, 2000; Luo *et al.*, 2008; Zhang, 2008, 2009, 2010; Zheng *et al.*, 2009), it does pose a challenge for simulation based surgery planning. Medialization laryngoplasty (Bielamowicz and Berke, 1995) is one surgical procedure, that is, particularly well suited for model-based surgical planning. The procedure is commonly used to restore voice in patients with unilateral vocal-fold paralysis/paresis and involves the insertion of a synthetic implant into the larynx via a window cut into the thyroid cartilage. A properly placed implant medializes the involved vocal fold, thereby leading to sustained vocal-fold vibrations and restoration of the voice. However, the surgical outcome is highly dependent on the shape, size and location of the implant, and the surgeon has few tools at hand that can predict the effect of different implant configurations on a given patient. A computational biomechanics based surgical planning tool could, therefore, significantly advance the surgical management of vocal fold paralysis/paresis and potentially improve surgical outcomes.

The level of fidelity required in such a surgical tool necessitates the use of sophisticated modeling approaches including continuum models for vocal fold mechanics (Alipour *et al.*, 2000; Rosa *et al.*, 2003; Zhang, 2008, 2009, 2010) and Navier-Stokes based glottal flow modeling (Luo *et al.*, 2008; Zheng *et al.*, 2009; Mihaescu *et al.*, 2010; Scherer *et al.*, 2010). Furthermore, simulations would have to be performed in patient-specific laryngeal models. In this regard, while the overall geometry of the lumen and the shape and size of the vocal folds can be obtained with reasonable accuracy from high-resolution CT scans (Jun *et al.*, 2005; Kim *et al.*, 2008), it is unlikely that patient-specific information regarding the layered internal structure can be extracted from these scans. Given this limitation, the only available option is to employ a model for the internal

[a)]Author to whom correspondence should be addressed. Electronic mail: mittal@jhu.edu

structure that can be considered prototypical for human adults. However, if such an approach is to be used, it is important to understand and quantify the sensitivity of the vibratory characteristics of the vocal folds to variations in the layered internal structure. Such an analysis would enable us to develop uncertainty (or "error") bounds for the simulations that are used for surgical planning in the future. This information could also potentially be useful in understanding the effect of aging and disease on phonation.

A variety of representations for the vocal fold inner layer have been employed in past studies. The simplest one among them is the single layer model which assumes the vocal fold to be composed of one kind of homogenous material and has been widely used in the past studies (Berry *et al.*, 1996; Cook *et al.*, 2007; Zhang *et al.*, 2007). More complex two (Hirano, 1974; Story and Titze, 1995) and three layer (Hirano, 1977) models also have been proposed in order to capture the vocal-fold vibration with higher fidelity. Studies have examined the effect of overall vocal fold size and shape on the vibratory mode (Cook *et al.*, 2007). However, to the best of our knowledge, no study to date has systematically examined and quantified the effect of the layered inner structure on the vibratory characteristics of the vocal folds. Such a study would help to create a unified foundation for understanding vibratory dynamics in computational models of phonation. Finally, such a study could also be useful in assessing the effect of factors such as age, gender and health on phonation.

A fully coupled fluid-structure interaction study (Rosa *et al.*, 2003; Luo *et al.*, 2008; Zheng *et al.*, 2009) between the vocal fold structure and airflow stream would enable a complete analysis of this issue. However, the computational expense of this approach coupled with the large parameter space that has to be covered make this prohibitive. A relatively inexpensive simple way to investigate this sensitivity is through an eigen analysis of the vocal folds. The superposition of eigenmodes provides a reasonable description of overall vibration patterns of vocal fold in normal human phonation (Moore and von Leden, 1958; Hirano, 1975; Berry *et al.*, 1994; Berry and Titze, 1996; Alipour *et al.*, 2000; Berry, 2001; Zhang *et al.*, 2007). In fact, the empirical eigenfunctions extracted from a fully coupled fluid-structure interaction simulation of vocal fold vibration also show a significant correspondence to the eigenmodes (Berry *et al.*, 1994; Berry *et al.*, 2001; Zhang *et al.*, 2006). Thus, a study of vocal fold eigenmodes and their sensitivity to the internal structure could provide insights that are useful in the development of simulation based tools for phonosurgery.

II. VOCAL FOLD MODEL

A. Baseline configuration

A three-dimensional idealized vocal fold model without longitudinal variation is employed as the baseline configuration in the current study. The overall shape of the vocal fold is based on the M5 profile of Scherer *et al.* (2001) and shown in Fig. 1(a). While this model is a significantly simplified representation of the human vocal folds, it has been widely used in phonation research (Scherer *et al.*, 2002; Shinwari *et al.*, 2003; Erath and Plesniak, 2006; Cook *et al.*, 2008, 2009).

The vocal fold model here is assumed to have a three-layer (cover-ligament-body) inner structure (Hirano *et al.*, 1981) [shown in Fig. 1(b)]. In this model, T_c and T_l are the thicknesses of cover and ligament layers, respectively, and for the baseline model, these are assumed to be constant through the superior, medial and inferior sections. Furthermore, L_1 and L_2 denote the length of the ligament in the coronal plane along inferior and superior surfaces, respectively.

The dimensions of the various layers for the nominal (baseline) model employed in this study are listed in Table I. The baseline model employs a longitudinally invariant inner structure and the nominal values (denoted by subscript "0") of the thicknesses of the cover and ligament are based on the measurements of Hirano *et al.* (1981). It should be noted that most 3D vocal-folds model have assumed such a longitudinally invariant inner structure (Alipour *et al.*, 2000; Tao and Jiang, 2007; Cook *et al.*, 2009).

The histological structure of the human vocal fold varies from individual to individual as well as with age, and variations are especially prominent in the ligament layer. For instance, newborns usually do not have a ligament layer and the ligament layer only develops gradually after the birth and becomes mature at puberty (Hirano *et al.*, 1981). A large variety of ligament layer models have been employed in the past studies. For instance, Alipour *et al.* (2000) only employed the

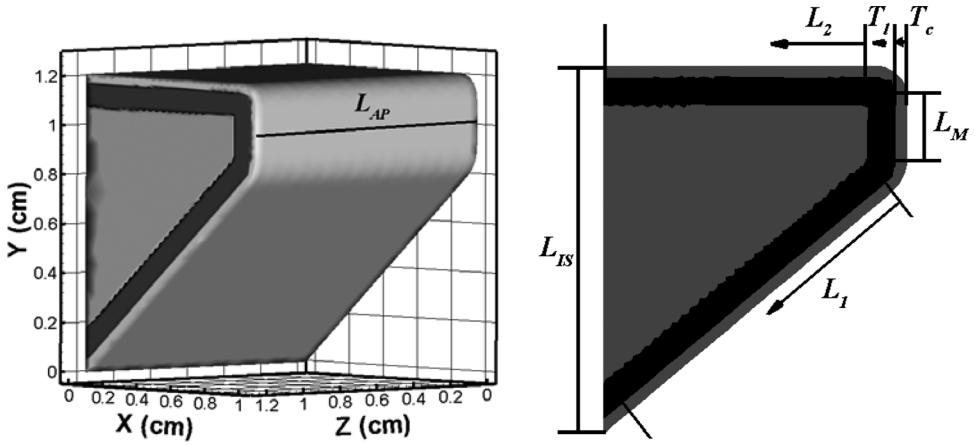

FIG. 1. Geometric model of vocal fold. (a) Three-dimensional vocal fold model; (b) Coronal cross section.

TABLE I. Dimension of the vocal fold and various layers for the nominal (baseline) models. Nominal values of dimensions that are varied in the current study are denoted by subscript "0."

Parameter	Symbol	Value (mm)
Vocal fold anterior-posterior length	L_{ap}	12
Vocal fold inferior-superior length	L_{is}	12
Thickness of cover layer	T_{c0}	0.33
Thickness of ligament layer	T_{l0}	1.11
Length of inferior ligament segment	$L10$	11.2
Length of superior ligament segment	$L20$	8.5
Length of medial ligament segment	L_M	2.75

medial segment to represent the whole ligament layer whereas Luo *et al.* (2008) have used a ligament model with both medial and inferior segments, as shown in Fig. 2(a) and 2(b), respectively. Still other studies have employed two-layer models [shown in Fig. 2(c)] that excluded a separate ligament layer (Story and Titze, 1995; Cook *et al.*, 2008, 2009; Zhang, 2009, 2010). Similarly, the cover is known to play an important role in sustaining the so-called mucosal wave, with direct implications for the quality and strength of the human voice. It is also well known that pathologies such as carcinomas, polyps, and nodules which change the structure of the cover are implicated in loss of voice. Additionally, surgical procedures that significantly modify the geometry of the cover (such as excessive bowing/stretching of the cover due to improperly placed thyroplasty implant) can lead to unsatisfactory surgical outcomes. All of these issues provide strong motivation for studying the effect of ligament size and cover thickness on vocal fold vibration. In human vocal folds, the thicknesses of the inner layers are known to vary along the longitudinal direction (Hirano *et al.*, 1981). Usually, the ligament layer is thicker at the sites of attachment at the anterior commissure and the vocal process of the arytenoid to withstand the massive stress of vocal fold action. The cover layer is thicker in the middle to provide a cushion for the vocal fold collision (Titze, 1994) and also to allow for adequate glottal opening during phonatory vibration. Figure 3(a) shows the thickness of each layer measured by Hirano *et al.* (1981). The locations of the points where the original measurements were made are represented by circles and we have fitted a fourth-order polynomial curve in order to get a smoothly varying curve for each layer. We note that the thicknesses of the cover and the

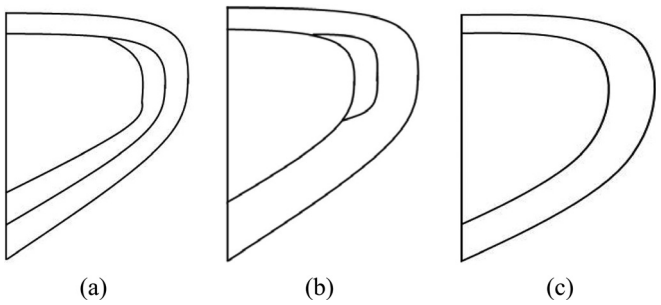

FIG. 2. Typical geometric models of vocal fold used in past studies. Three-layer model from (a) Luo *et al.* (2008); (b) Alipour *et al.* (2000). The three layers are the cover, the ligament and body (vocalis). (c) two-layer (body-cover) model from Cook *et al.* (2008, 2009).

ligament vary in the longitudinal direction by up to 61% and 43%, respectively, about their nominal values, and these are relatively large variations which could have a significant impact on the vocal-fold vibration.

The three-dimensional topology of the vocal fold, where the inner structure is based on Hirano's measurements, is illustrated in Fig. 3(b). In this model, the nominal thickness of cover and ligament layers (listed in Table I) are the average value of the measurements by Hirano *et al.* (1981). We denote this model as the "Hirano Model" for the purposes of the current study.

The current study begins with a modal analysis of the "Hirano Model." along with two other distinct models: the model with ligament only on the medial surface [Fig. 2(b)] and the two-layer model [Fig. 2(c)]. The results of these models are compared to the baseline model to assess the effects of longitudinal variation in the sublayers as well as large scale changes in the ligament layer on the vibratory characteristics of the vocal fold.

B. Material properties

In general, vocal fold tissue exhibits a nonlinear stress-strain relationship (Min *et al.*, 1995; Chan and Titze, 1999; Zhang *et al.*, 2006). However, this nonlinearity becomes obvious only during large deformation events such as posturing or implant insertion. Due to the small strain and displacement produced, the vocal folds can be modeled as linear materials during phonation (Cook *et al.*, 2008). In addition, vocal fold tissue is considered as an incompressible material

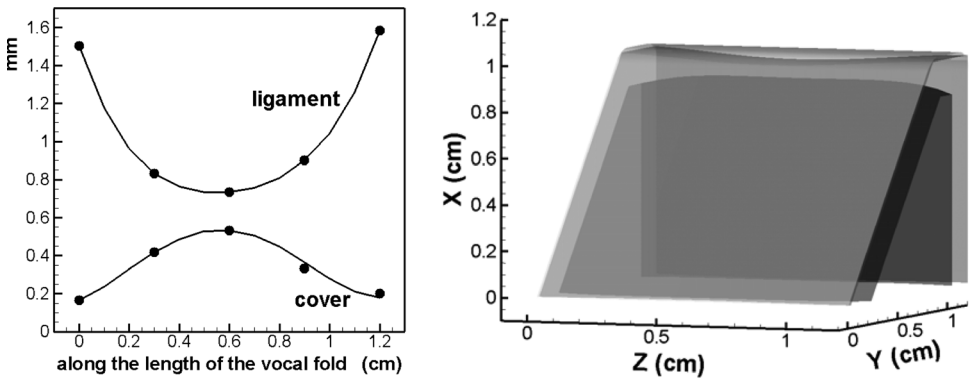

FIG. 3. Vocal fold geometric model with longitudinal variation in layer thickness, i.e., the "Hirano Model." (a) Longitudinal variation of the thicknesses of the cover and ligament layers based on the measurements of Hirano *et al.* (1981) which are represented by •; (b) the three-dimensional "Hirano Model" model based on thickness variations shown in (a).

TABLE II. Material properties assumed for the three layers in the current study. All values (except for the Poisson's ratio) are in kilo-Pascals (kPa).

Property	Value		
	Cover	Ligament	Muscle
Transverse Young's modulus	2.0	3.3	4.0
Longitudinal shear modulus	10	40	12
Longitudinal Young's modulus	20140	33060	39900
Transverse Poisson's ratio	0.9	0.9	0.9

because it consists mostly of water (Berry and Titze, 1996). In the current study, all three layers of vocal fold tissue were modeled as linear elastic, transverse isotropic and nearly incompressible material. The assumption of "nearly incompressible" was used to avoid a singularity in the compliance matrix (Cook *et al.*, 2008).

The material properties assumed for the three layers of the vocal-fold are also listed in Table II. Note that the longitudinal Young's modulus for all of three layers is 10^4 times the transverse Young's modulus to satisfy the in-plane motion assumption (Cook *et al.*, 2008). It should also be noted that there is considerable uncertainty about these material properties and this also has implications for simulation based phonosurgery planning tools. However, there are substantial efforts ongoing to better characterize the material properties (Chan and Titze, 1999, 2000; Chan, 2001, 2004; Min, 1996; Philips *et al.*, 2009) and the sensitivity of the vocal fold vibration to these properties has been studied in detail by Cook *et al.* (2009). Given this, we have not explored this aspect further in the current study but have instead, assumed properties that are relatively well supported by past studies.

C. Computational method

The equations governing the vocal-fold vibration are the Navier equations (Fung, 1965) which are given by

$$\nabla \cdot \sigma + \rho f = \rho \frac{d^2 u}{dt},$$

where σ is the stress tensor, $\boldsymbol{f}$ is the body force vector, ρ is the density, and $\boldsymbol{u}$ is the displacement vector. Fixed (zero displacement) boundary conditions are imposed on the lateral, anterior and posterior surfaces, while traction-free boundary conditions are imposed on the medial, superior, and inferior surfaces. A Galerkin finite-element method is employed for discretizing the above equations and the discretized equations are reformulated into the following eigenvalue problem (Everstine, 2008):

$$\boldsymbol{K} \cdot \boldsymbol{u}_0 = \omega^2 \boldsymbol{M} \cdot \boldsymbol{u}_0,$$

where $\boldsymbol{M}$ and $\boldsymbol{K}$ are the mass and stiffness matrices respectively, $\boldsymbol{u_0}$ is the displacement eigenmode and ω is the natural frequency. Since vocal fold contact and other interactions between the two vocal folds cannot be included in the eigenanalysis, we only discretize and study a single vocal fold.

In the current study, a high-density tetrahedral grid with about 23 thousand elements is used to discretize the vocal fold. This high grid density is required in order to adequately resolve the subtle effect of the geometry of the various layers. As shown in Fig. 4, elements are clustered in and around the cover and ligament layers to provide higher resolution for accurately capturing these effects. The eigenvalue problem is solved using Gram-Schmidt orthogonalization (Everstine, 2008), and we have performed a grid-dependency to ensure that the first six computed eigenmodes are independent of the grid. Further details about the finite-element formulation can be found in Zheng (2009). Fully converged solutions for the eigenmodes require up to 10 h of computational time per configuration on a high-end workstation.

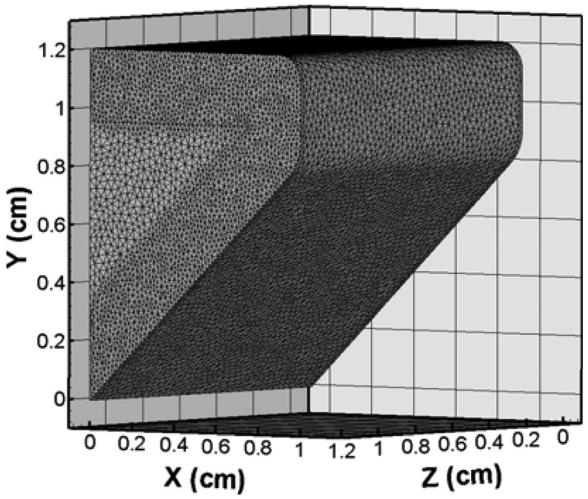

FIG. 4. Volume mesh employed in eigenanalysis.

III. MODEL STUDIES

Eigenanalysis is first performed on the baseline and Hirano models to investigate the effect of inner structure anterior-posterior variation on the vibratory characteristics of the vocal folds. Two other distinct models, the "two-layer model" in which ligament layer is assumed to be absent (Story and Titze, 1995; Cook *et al.*, 2008, 2009), and the "medial ligament model" where the ligament is limited to a small region near the median (Alipour *et al.*, 2000; Tao and Jiang, 2007), are also included in our initial comparative analysis.

Subsequent to this initial set of cases, two sets of models are analyzed to study the effect of the ligament layer configuration and thickness of cover and ligament layers. As in the rest of the study, the material properties and overall vocal fold dimensions are kept the same for all the models. The layered model of the vocal fold is defined by four geometric parameters: L_1, L_2, T_c and T_l as shown in Fig. 1(b). By changing the value of each of these parameters in a range about the baseline value, twenty-eight separate vocal fold configurations were created. In most cases only one parameter was varied at a time with the other parameters held fixed at their nominal values. For one set of models we vary L_1 and L_2 simultaneously and for these, choosing $L_1 = L_2 = 0$ leads to what we refer to as the "medial ligament model." It should be noted that changes in the dimensions of the cover and ligament layers are accommodated by concomitant changes in the muscle in order to ensure that the overall size of the

TABLE III. Parameter ranges and schematics of inner structure of the vocal fold models employed in the current study.

Model	Parameter(s) varied	Parameter range (nominal value (mm))	Schematic of resultant vocal fold
Baseline model	None	N/A	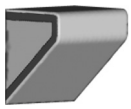
Hirano Model	Longitudinally varying ligament and cover thickness	N/A	
Length of ligament layer along superior and inferior surfaces	L_1	0–100% (11.2)	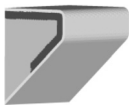
	L_2	0–100% (8.5)	
	L_1 and L_2 (varied simultaneously)	0–100% (11.2 & 8.5)	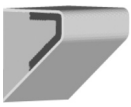
Cover and ligament thickness	T_c	50%–300% (0.33)	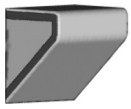
	T_l	0–200% (1.11)	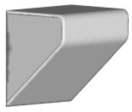

vocal fold is held invariant. The parameter ranges as well as schematics of layered structure of vocal fold for these 28 cases are summarized in Table III.

IV. RESULT AND DISCUSSION

A. Modal analysis for four distinct models

Four distinct models, which are the baseline model, the Hirano model, the medial ligament ($L_1 = 0$ and $L_2 = 0$) and the two-layer model ($T_l = 0$), were selected first to investigate the effect of large-scale structural variations on the vocal fold vibration. It should be noted that while FEM based models such as the one employed here produce a large number of eigenmodes, past studies (Titze, 1988; Berry *et al.*, 1994; Berry and Titze, 1996) have shown that vocal fold vibration during phonation is sufficiently well described by a combination of the first few eigenmodes. Thus, in comparing the vocal fold vibratory characteristics for the various models, we focus on the first four eigenmodes.

The four lowest eigenfrequencies and corresponding eigenmodes computed for these four models are shown in Table IV. Corresponding two dimensional mid-coronal views at two extreme phases are also shown in Table IV. In general, it is noted that the baseline, Hirano and medial ligament models, which vary significantly in their inner structure, exhibit modal shapes that are qualitatively similar. The first eigenmode (Mode-1) corresponds to a strong vertical motion occurring primarily on the superior and inferior surfaces. The second mode (Mode-2) presents a lateral motion with a slight phase difference between the inferior and superior surfaces. The third mode (Mode-3) is a vertical motion of the whole vocal fold. Finally, in Mode-4, the majority of motion only occurs at the tip region of the superior surface and it contributes to the formation of the distinct convergent-divergent glottal shape. It should be noted that although some degree of glottal convergence-divergence can be observed in all of the four modes, it is most prominent in Mode-4.

The two-layer model however exhibits large dissimilarities to the other three models in terms of the eigenmodes. However, a comparison of the eigenmodes of the two-layer model with all the four eigenmodes of other three models indicates that many of these differences are associated with a change in the modal-order. For instance, Mode-1 of the two layer model presents a vertical motion of the whole vocal fold which is similar to Mode-3 of the other three models. The only difference in the modal shape is that that the two-layer model has a more smooth deformation on the superior and inferior surfaces. Mode-2 of the two-layer model shows similarities to both Mode-1 and Mode-4 of other three models with a clear vertical motion on the superior and inferior surfaces as well as a noticeable deformation around the superior tip region. Similarly, Mode-3 of the two-layer model is observed to be mostly similar to Mode-2 of the other models; the mode has a lateral motion of the vocal fold and slight phase difference between the superior and inferior surfaces. The modal shape of Mode-4 of the two-layer model remains highly similar to the corresponding mode of other models.

TABLE IV. Four lowest eigenmodes and corresponding eigenfrequencies for four models. The solid and dash lines represent two phases in the eigenmodes at the longitudinal midplane.

	Baseline model	Hirano Model	Medial Ligament Model	Two-Layer Model
	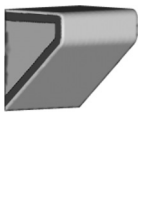	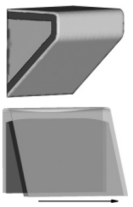	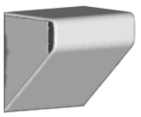	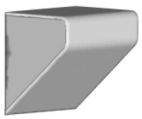
Mode 1	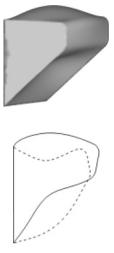	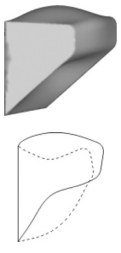	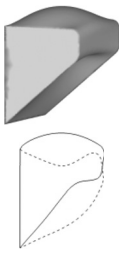	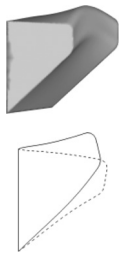
	184Hz	187Hz	151Hz	144Hz
Mode 2	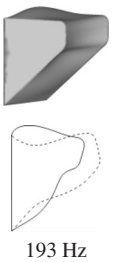	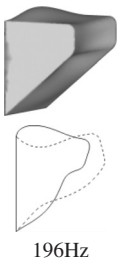	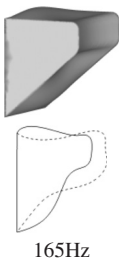	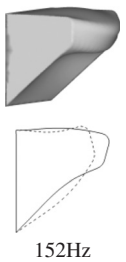
	193 Hz	196Hz	165Hz	152Hz
Mode 3	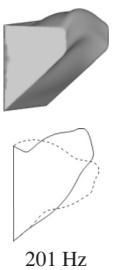	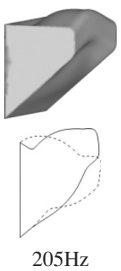	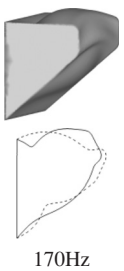	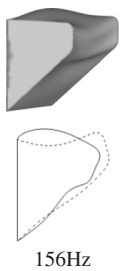
	201 Hz	205Hz	170Hz	156Hz
Mode 4	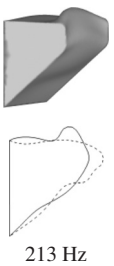	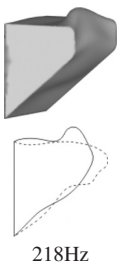	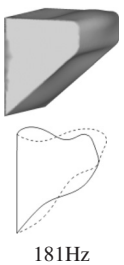	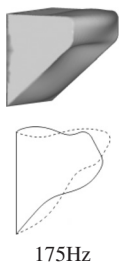
	213 Hz	218Hz	181Hz	175Hz

One interesting finding from this close examination is that more superior-inferior phase difference appears in the lower order modes in the two-layer model. This has implication for vocal fold modeling in that it suggests that reducing/removing the ligament layer can potentially enhance the formation of a convergent-divergent glottal shape.

In order to more precisely quantify the similarity of the modal shapes for the various models, we compute dot-products between the eigenvectors for the different models. This is done as follows: the *j*th eigenmode is written into a single vector $\vec{q}_j = \left(u_{j1}, v_{j1}, w_{j1}, \ldots, u_{jN}, v_{jN}, w_{jN}\right)$, where u_{jm}, v_{jm}, and w_{jm} represent the displacements of the *m*th grid point in the x, y, and z directions, respectively, for the *j*th eigenmode. This vector is normalized with its own magnitude leading to a normalized vector: $\vec{Q}_j = \vec{q}_j / |\vec{q}_j|$, where $|\vec{q}_j| = \sqrt{\sum_{i=1}^{N} u_{ji}^2 + v_{ji}^2 + w_{ji}^2}$ and N is the total number of grid points. The dot-product of any two normalized eigenmodes (denoted by π) is indicative of the similarity between the two modes with a dot-product value of one corresponding to an exact match, and zero indicating complete orthogonality.

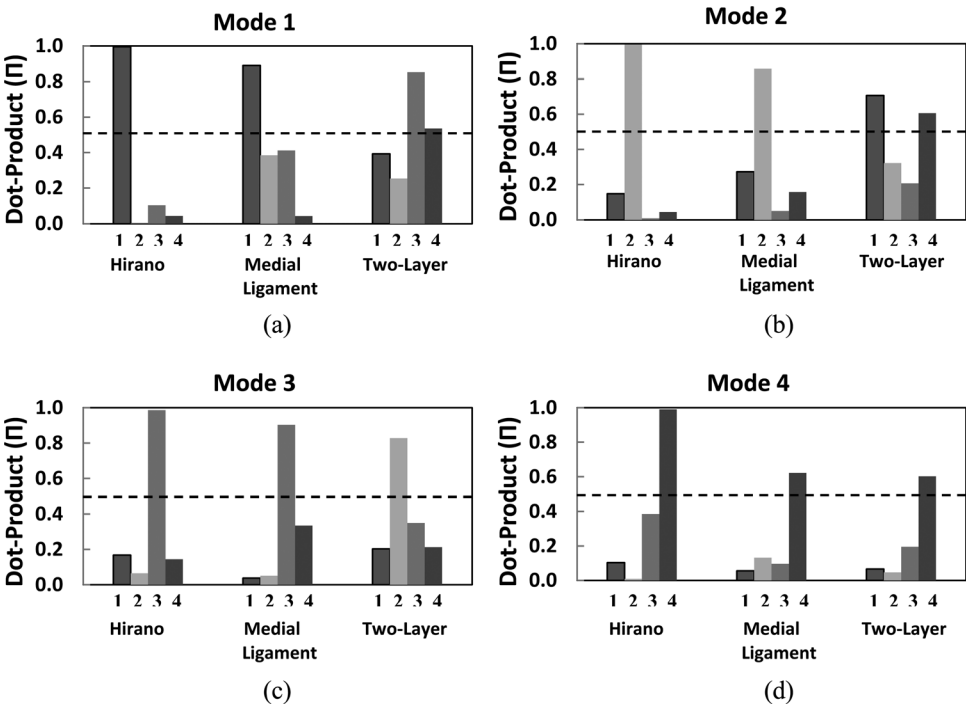

FIG. 5. Dot-product between eigenmodes of the three models and each baseline mode. Each plot corresponds to one particular eigenmode of the given model and the numbers 1–4 on the abscissa correspond to the four baseline modes.

In the rest of the paper, the four eigenmodes of the baseline model are referred to as baseline modes. Figure 5(a) displays the dot-products between Mode-1 of the three variant models (Hirano model, medial ligament model, and two-layer model) and the four baseline modes. The numbers from 1 to 4 on the abscissa refer to the corresponding baseline modes. Figures 5(b), 5(c), and 5(d) show the corresponding plots for Modes-2, 3, and 4, respectively. It should be noted that while eigenmodes for a given model are orthogonal to each other, modes for different models do not have to be orthogonal. Thus, dot-products between modes of different models can range anywhere from 0 to 1 and furthermore, a given mode might have significant similarity with more than one baseline mode. In the current study, we choose a criterion that two modes are similar if the dot-product between them is greater than 0.5. While the choice of the cut-off value is *ad hoc,* it is reasonably in-line with the notion of similarity. The dot-products of the first four eigenmodes of the various models to the four baseline modes are presented in Table V.

This analysis shows that the Hirano model has vibratory modes that are nearly identical to the corresponding baseline modes; the modal order is preserved and the dot-products between the corresponding modes are found to vary from 0.986 to 0.996. In addition, the lowest four eigenfrequencies (shown in Table IV) are within 5 Hz of the ones for the baseline model which represents at most a 2.3% variation over the baseline values. Therefore, vocal fold models with longitudinal variation in the thicknesses of cover and ligament layers that nominally matches Hirano's measurement, produce vibratory modes that are virtually identical to a longitudinally invariant model with thicknesses corresponding to the longitudinally averaged values. The current study therefore shows that from a dynamical point-of-view, including a longitudinal variation in the thicknesses of the various vocal fold layers is not essential. In the rest of the paper, we therefore focus only on longitudinally invariant models.

Analysis also shows that the medial ligament model has the same modal order as the baseline model. Regarding the modal shape, the first three eigenmodes are highly similar to the corresponding baseline modes with dot-products ranging from 0.85 to 0.9. The reduced similarity of Mode-4 with the corresponding baseline mode is confirmed by a dot-product of only 0.622. A significant reduction (around 30 Hz) in the eigenfrequencies is also found for the medial ligament model.

Our earlier observations about the shape change of eigenmodes of the two-layer model can be explained quantitatively by Table V. Generally, the first four eigenmodes of the two-layer model are still similar in shape with the baseline model with dot-product varying from 0.602 to 0.882. However, the modal order of modes in this new model is

TABLE V. Similarity of the first four modes of the various models to the four baseline modes. Each cell in the table shows which baseline mode(s) is (are) similar to each mode for a given model.

Model↓	Mode →	Mode 1 (Π)	Mode 2 (Π)	Mode 3 (Π)	Mode 4 (Π)
Hirano		1 (0.996)	2 (0.996)	3 (0.986)	4 (0.990)
Medial Ligament		1 (0.890)	2 (0.859)	3 (0.903)	4 (0.622)
Two-Layer		3 (0.882)	1 (0.707)	2 (0.828)	4 (0.602)
		4 (0.536)	4 (0.607)		

quite different. Mode-1 of the two-layer model is found to be highly similar to baseline Mode-3 and Mode-4 with dot-products of 0.882 and 0.536, respectively. Mode-2 is highly similar to baseline Mode-1 and Mode-4 with dot-products of 0.707 and 0.607, respectively. Mode-3 is found to be most similar to baseline Mode-2 with a dot-product of 0.828 whereas Mode-4 is most similar to the corresponding baseline mode with a dot-product of 0.602. Interestingly, Modes-1, 2, and 4 show nearly the same level of similarity with baseline Mode-4. Thus with respect to the modal shapes, the primary effect of ligament removal is a rearrangement and redistribution of shapes within the four modes. It should also be noted that the overall modal frequency drops by about 40 Hz for the modes of the two-layer models as compared to the baseline model.

B. Effect of ligament length

The previous section indicates that a significant reduction in the length of the ligament layer has a noticeable effect on the eigenfrequencies and this motivates a closer examination of the effect of ligament length on the vocal fold vibratory modes. In the current study this is accomplished by varying L_1 (length of inferior ligament segment) and L_2 (length of superior ligament segment) individually as well as simultaneously. When one length parameter is varied, the other one is kept at its maximum (baseline) value whereas when both are varied simultaneously, they are varied by the same relative value. The values of L_1 or L_2 in the various cases, range from 0% to 100% of their maximum (baseline) values. If we define the total length of the ligament for any given case as $L_T = L_1 + L_2 + L_M$ and the total length of the baseline case as $L_{T0} = L_{10} + L_{20} + L_M$, the values of L_T/L_{T0} then vary from 50% to 100% for case where L_1 is varied, from 62% to 100%when L_2 is varied, and from 12% to 100% when L_1 and L_2 are varied simultaneously.

As found for the medial-ligament model, even significant reductions in ligament length do not change the modal structure and order of the four lowest eigenmodes and each of the four modes continues to match best the corresponding baseline modes. Given this, we can examine the variation of frequency of each mode with ligament length. Figure 6. shows the eigenfrequencies for the first and fourth modes plotted versus against L_T/L_{T0} for the three different cases. The figure shows that the eigenfrequencies of Mode-1 and Mode-4 (Mode-2 and 3 excluded since they show similar behavior) decrease monotonically with a reduction in ligament length in all three models and they share a similar pattern of decrease; they are relatively insensitive to an initial reduction, but then reduce more rapidly with further reductions in ligament length. The range of relative insensitivity extends up to 25% reduction for the model for which only $L1$ is reduced, as well as for the model where both L_1 and L_2 are reduced simultaneously. For the model where only L_2 is reduced, this range extends only up to 10% reduction. It is also noted that the model with variation in only L_2 show the highest rate of decrease in this latter range.

The sensitivity of the eigenfrequencies to ligament length is further quantified by computing the overall relative change in eigenfrequency over the overall relative change in total ligament length, i.e., $(\Delta f/f_0)/(\Delta L_T/L_{T0})$. Within the context of control theory such a parameter is also called a control coefficient (Kacser and Burns, 1995; Heinrich and Rapoport, 1974). These values are summarized in Table VI. The highest value for this quantity is found to be 0.28 which indicates that a 1% change in ligament length leads to at most a 0.28% change in eigenfrequency. This relative insensitivity of the frequency bodes well for computational modeling of phonation since it implies that uncertainties in the ligament length are expected to translate to lower magnitudes of uncertainties in the predicted eigenfrequencies.

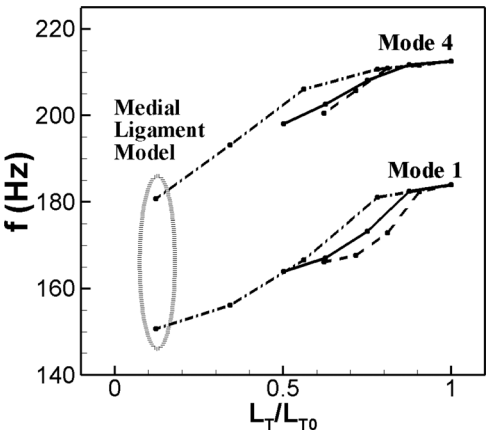

FIG. 6. Eigenfrequencies for the first and fourth modes plotted versus L_T/L_{T0} for the three different cases. (solid line) Only L_1 is reduced; (dashed line) only L_1 is reduced; (dot dashed line) both L_1 and L_2 are reduced simultaneously.

C. Effect of ligament and cover layer thickness

Another structural feature of the vocal fold which potentially plays an important role in the vocal fold vibration but cannot be reliably extracted from CT and other modalities is the thickness of the cover and ligament layers. In order to explore the sensitivity of the VF vibration to this feature, we have systematically examined the dependence of eigenfrequencies on the thicknesses of the ligament and cover layers. As shown in Table III, the thicknesses of the cover and ligament layers were varied in a range of 50%–300% and 0–200%, respectively, of the baseline values. When one of them is changed, the other one is kept constant at the baseline value and the muscle thickness adjusted to maintain a constant total volume.

The effect of changes in the thickness of cover and ligament layers on the modal shape is analyzed first by computing dot-products with baseline modes and this data is presented in Table VII. It is found that for a cover layer

TABLE VI. Relative change in eigenfrequency normalized by relative change in total ligament length $(\Delta f/f_0)/(\Delta L_T/L_{T0})$.

Parameter Varied	Mode-1	Mode-2	Mode-3	Mode-4
L_1	0.22	0.22	0.20	0.14
L_2	0.26	0.28	0.26	0.15
L_1 & L_2	0.21	0.16	0.18	0.17

TABLE VII. Similarity of the first four modes to four baseline modes in models with different cover layer thickness. Each cell in the table shows which baseline mode(s) is(are) most similar to each mode for a given model.

$T_C/T_{C0}\downarrow$	Mode →	Mode 1 (Π)	Mode 2 (Π)	Mode 3 (Π)	Mode 4 (Π)
0.5		1 (0.996)	2 (0.996)	3 (0.949)	4 (0.717)
1.0		1 (1.000)	2 (1.000)	3 (1.000)	4 (1.000)
1.5		1 (0.989)	4 (0.799)	2 (0.984)	4 (0.668)
			3 (0.765)		
2.0		4 (0.855)	1 (0.965)	2 (0.885)	3 (0.537)
		3 (0.671)			
2.5		4 (0.858)	1 (0.709)	2 (0.749)	?
		3 (0.671)			
3.0		4 (0.850)	?	1 (0.721)	?
		3 (0.687)		2 (0.593)	

thickness which is up to 50% below the nominal value, the modal shape of each eigenmode is approximately identical to the baseline model. However, when the thickness is increased to 1.5 times of the nominal value, Mode-2 shows significant similarity with the fourth and third baseline modes; after the thickness reaches two times of the nominal value, the fourth baseline mode becomes the first eigenmodes of these models and the dot product remains at a constant value of around 0.85. It should also be noted that for high values of cover thickness, there are some modes (such as Mode-4 for $T_C/T_{C0} = 2.5$ and Modes-2 and 4 for $T_C/T_{C0} = 3.0$) which do not show significant similarity to any of the four baseline modes. For these cases, one possibility is that these modes are similar to some higher (>4) baseline mode(s); the other possibility is that they are not similar to any particular baseline mode.

Table VIII shows the behavior of the models for different ligament thicknesses. For ligament thicknesses T_l/T_{l0} varying between 0.2 and 1.5 the modal order remains relatively unchanged from that of the baseline model. This indicates that for a relatively large range of ligament thicknesses, the vibratory modes remain qualitatively the same. For the two-layer model for which the ligament thickness is zero, the first, second, and fourth eigenmodes present high similarity with baseline Mode-4. Given that baseline Mode-4 corresponds to a converging-diverging glottal shape, the current results suggest that a thinner ligament facilitates the appearance of a converging/diverging mode. It should be noted that thickening cover layer and thinning the ligament layer leads to an overall decrease in the peripheral stiffness of the vocal fold since the ligament is stiffer than the cover. However, as shown in the previous section, reduction in ligament length, which would also decrease peripheral stiffness, does not have a similar effect. Thus the change in modal order and the appearance of the converging-diverging mode seems to specifically linked to the change in the thickness of the ligament layer.

Figure 7 shows the relationships between the lowest four eigenfrequencies and the ligament and cover layer thicknesses. The observed behavior can be explained by noting that the transverse Young's modulus and longitudinal shear modulus are the key determinants of overall material stiffness for the linearly elastic transversely isotropic material with constrained longitudinal motion (Cook *et al.*, 2008). The longitudinal shear modulus of each layer employed in the current study is much higher than the transverse Young's modulus (Alipour *et al.*, 2000). Furthermore, among the three layers, the ligament is assumed to have the highest longitudinal shear modulus; almost four times the value of the other two layers. Thus, the ligament layer presents the highest overall stiffness compared to the cover and muscle layers. Consequently, as the ligament layer is thickened and the muscle thickness decreased correspondingly, the overall stiffness of the vocal-fold increases thereby leading to an increase in the eigenfrequencies. It should be noted that the model topology reduces to that of a typical two-layer model as $T_l/T_{l0} = 0$ and the lowest four eigenfrequencies reduce by about 25% compared to the three-layer model with $T_l/T_{l0} = 1$.

TABLE VIII. Similarity of the first four modes to four baseline modes in models with ligament layer thickness variation. Each cell in the table shows which baseline mode(s) is(are) most similar to each mode for a given model.

$T_l/T_{l0}\downarrow$	Mode →	Mode 1 (Π)	Mode 2 (Π)	Mode 3 (Π)	Mode 4 (Π)
0.0		3 (0.852)	1 (0.707)	2 (0.828)	4 (0.602)
		4 (0.536)	4 (0.607)		
0.2		1 (0.785)	2 (0.695)	3 (0.767)	4 (0.786)
		3 (0.624)			
0.4		1 (0.920)	2 (0.900)	3 (0.932)	4 (0.870)
1.0		1 (1.000)	2 (1.000)	3 (1.000)	4 (1.000)
1.5		1 (0.982)	2 (0.965)	3 (0.834)	4 (0.843)
				4 (0.725)	
2.0		1 (0.885)	4 (0.849)	2 (0.947)	3 (0.584)
			3 (0.665)		

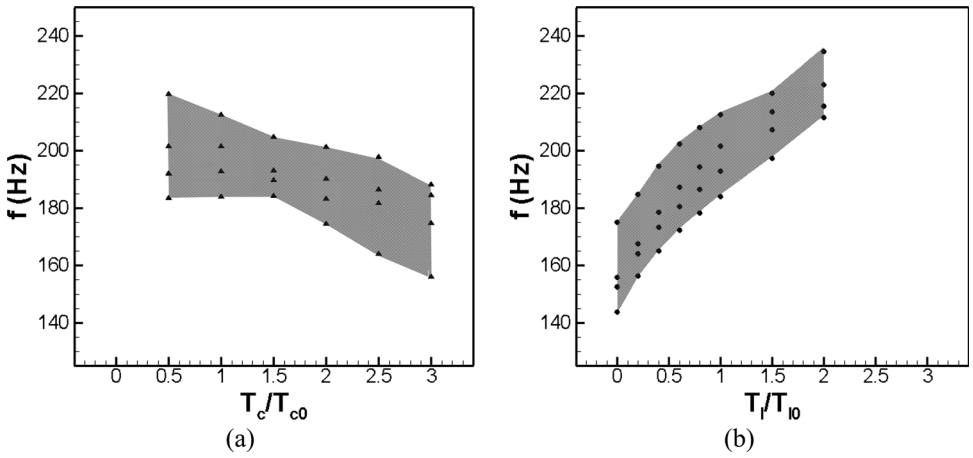

FIG. 7. Variation of the first four eigenfrequencies for models with thickness change in (a) cover layer and (b) ligament layer.

Similar to the previous section, the normalized change of eigenfrequencies per normalized change in layer thickness is computed to quantify the sensitivity to these features and the results are shown in Table IX. We find that Mode-2 and Mode-3 are equally sensitive to the thickness change in either cover or ligament layer. Mode-1 and Mode-4 appear to be more sensitive than Mode-2 and Mode-3 to the thickness change in cover layer, while for changes in the ligament layer, higher eigenfrequencies are always less sensitive than the lower ones. The highest sensitivity is 0.18 which implies a 0.18% change in frequency for a 1% change of thickness. This indicates a high level of insensitivity of the eigenfrequencies to the thicknesses of the cover and ligament.

V. SUMMARY AND CONCLUSIONS

A parametric eigen-analysis has been carried out to investigate the effect of the inner multilayer structure of the vocal folds on the vibratory dynamics. The baseline vocal fold model chosen is a three-layer model with cover, ligament, and muscle and the model is discretized using a high-resolution finite-element method. A wide range of features, which include the longitudinal variation in layer thickness, ligament length, and cover and ligament thickness, are varied and the first four eigenmodes and eigenfrequencies are compared to the baseline model. Several key observations and conclusions can be drawn from the results:

(1) The vibratory modes are quite insensitive to thickness variation of the layers along the longitudinal direction—the type that is considered typical for human adults (Hirano *et al.*, 1981). Therefore, assuming a longitudinally invariant layer structure in computational solid dynamics models of vocal folds should be acceptable.

TABLE IX. Changing rate of eigenfrequencies over the relative change of thicknesses in both cover and ligament layers normalized by eigenfrequencies of baseline case (%/%).

Parameter Varied	Mode-1	Mode-2	Mode-3	Mode-4
T_c	−0.06	−0.04	−0.05	−0.06
T_l	0.18	0.16	0.16	0.14

(2) Significant reduction in ligament length, even all the way down to the medial ligament model where the ligament is limited to a small section near the superior tip of the vocal fold, does not qualitatively change the eigenmodes or the modal order. The eigenfrequency, however, decreases monotonically with decreasing ligament length. The rate of decrease is not large in that a 10% uncertainty in eigenfrequency (which would be considered acceptable in a computational model) would require at least a 35% uncertainty in ligament length.
(3) While significant (up to 50%) decrease in the cover thickness has no qualitative effect on the eigenmodes, increase in cover thickness tends to change the modal order with the lower modes showing a greater resemblance to the higher baseline modes and vice-versa. Given that the baseline Mode-4 has a strong converging-diverging (mucosal-wave type) behavior, this leads to the conclusion that increase in cover thickness enhances the tendency for mucosal wave formation.
(4) Up to a 50% decrease in ligament thickness does not result in significant changes in the modal structure order. Further decrease tends to modify the modal order with the zero-thickness case (two-layer model) exhibiting the mucosal-wave mode as the first mode. This observation is consistent with the behavior seen for increasing cover thickness.
(5) Significant ($>50\%$) increase in ligament thickness leads to a different behavior. While Mode-1 retains its position in the modal order, baseline Mode-4 moves up in the modal order to become the second mode for these models. Thus, a thick ligament would also increase the tendency of the vocal folds to show a converging-diverging behavior. Thus, the effect of the ligament thickness is non-monotonic in that both very thick as well as very thin ligaments promote the appearance of converging-diverging type of vibratory behavior.
(6) The overall sensitivity of eigenfrequencies to the cover and ligament thicknesses is quite small with a 10% uncertainty in eigenfrequency requiring at least a 55% uncertainty in the layer thicknesses.

In summary, the overall conclusion regarding the feasibility of accurate computational modeling of phonation in

the face of relatively high levels of uncertainty regarding the inner structure is generally positive. Longitudinal variations in layer thickness can be ignored and even large relative changes in ligament length and ligament and cover thickness produce few qualitative differences. However, some reasonable measures of these parameters are required in order to enable realistic modeling of the vocal fold dynamics. Furthermore, the current study also shows that radically different models (such as the two-layer model) could possibly exhibit quite different dynamics, and therefore, care needs to be taken in interpreting the results from any particular model.

Finally, it is useful to point out the caveats and limitations of the current study. First, all the models in the current study assume the same overall vocal fold shape (based on the M5 model of Scherer *et al*., 2001) as well as material properties for the body, ligament, and cover layers. As shown by Cook *et al*. (2007, 2009), these features/properties also have a significant effect on the modal structure of the eigenmodes. Thus, the conclusions reached in the current study might be further confounded by changes in these other features. It should be noted that several ongoing studies are attempting to accurately measure the material properties of vocal folds (Chan, 2004; Titze *et al*., 2004; Klemuk and Titze, 2004; Chan and Titze, 2006; Goodyer *et al*., 2006, 2007a, 2007b, 2009; Chan and Rodriguez, 2008), and this should reduce the uncertainty associated with this aspect in the future.

The second limitation is associated with the use of eigenmodes as a proxy for assessing the vibratory dynamics. While linear eigenmodes do provide useful information about the vibratory dynamics, it is well known that other effects, such as mode entrainment, are manifested in the presence of non-linear effects associated with flow coupling and vocal fold contact. These effects can only be included by performing full fluid-structure interaction simulations for all these models.

The computational expense of such a study, however, make it infeasible at the present time. Thus, care needs to be taken in extrapolating the conclusions of the current study to fully coupled fluid-structure interaction models of phonation.

ACKNOWLEGEMENTS

The project described was supported by Grant Number ROIDC007125 from the National Institute on Deafness and Other Communication Disorders (NIDCD). The content is solely the responsibility of the authors and does not necessarily represent the official views of the NIDCD or the NIH. This research was also supported in part by the National Science Foundation through TeraGrid resources provided by NICS under grant number TG-CTS100002.

Alipour, F., and Titze, I. R. (**1991**). "Elastic models of vocal fold tissues," J. Acoust. Soc. Am. **90**(3), 1326–1331.

Alipour, F., Berry, D. A., and Titze, I. R. (**2000**). "A finite-element model of vocal-fold vibration," J. Acoust. Soc. Am. **108**(6), 3003–3012.

Chan, R. W. (**2004**). "Measurements of vocal fold tissue viscoelasticity: Approaching the male phonatory frequency range," J. Acoust. Soc. Am. **115**(6), 3161-3170.

Berry, D. A., Montequin, D. W., and Tayama, N. (**2001**). "High-speed digital imaging of the medial surface of the vocal folds," J. Acoust. Soc. Am. **110**(5), 2539–2547.

Berry, D. A., Herzel, H., Titze, I. G., and Krischer, K. (**1994**). "Interpretation of biomechanical simulations of normal and chaotic vocal fold oscillations with empirical eigenfunctions," J. Acoust. Soc. Am. **95**(6), 3595–3604.

Berry, D. A., and Titze, I. R. (**1996**). "Normal modes in a continuum model of vocal fold tissues," J. Acoust. Soc. Am. **100**(5), 3345–3354.

Berry, D. A. (**2001**). "Mechanisms of modal and nonmodal phonation," J. Phonetics **29**, 431–450.

Bielamowicz, S., and Berke, G. B. (**1995**). "An improved method of medialization laryngoplasty using a three-sided thyroplasty window," Laryngoscope **105**(5), 537–539.

Chan, R. W. (**2004**). "Measurement of vocal fold tissue viscoelastic: approaching the male phonatory frequency range," J. Acoust. Soc. Am. **115**(6), 3161–3170.

Chan, R. W. (**2001**). "Estimation of viscoelastic shear properties of vocal-fold tissues based on time-temperature superposition," J. Acoust. Soc. Am. **110**(3), 1548–1561.

Chan, R. W., and Titze, I. R. (**1999**). "Viscoelastic shear properties of human vocal fold mucosa measurement methodology and empirical results," J. Acoust. Soc. Am. **106**(4), 2008–2021.

Chan, R. W., and Titze, I. R. (**2000**). "Viscoelastic shear properties of human vocal fold mucosa: Theoretical characterization based on constitutive modeling," J. Acoust. Soc. Am. **107**(1), 565–580.

Chan, R. W., and Titze, I. R. (**2006**). "Dependence of phonation threshold pressure on vocal tract acoustics and vocal fold tissue mechanics," J. Acoust. Soc. Am. **119**, 2351–2362.

Chan, R. W., and Rodriguez, M. L. (**2008**). "A simple-shear theometer for linear viscoelastic characterization of vocal fold tissues at phonatory frequencies," J. Acoust. Soc. Am. **124**(2), 1207–1219.

Cook, D. D., Nauman, E., and Mongeau, L. (**2007**). "Sensitivity of a continuum vocal fold model to geometric parameters, constraints and boundary condtions," J. Acoust. Soc. Am. **121**(4), 2247–2253.

Cook, D. D., Nauman, E., and Mongeau, L. (**2008**). "Reducing the number of vocal fold mechanical tissue properties: Evaluation of the incompressibility and planar displacement assumptions," J. Acoust. Soc. Am. **124**(6), 3888–3896.

Cook, D. D., Nauman, E., and Mongeau, L. (**2009**). "Ranking vocal fold model parameters by their influence on modal frequencies," J. Acoust. Soc. Am. **126**(4), 2002–2010.

Erath, B. D., and Plesniak, M. W. (**2006**). "An investigation of bimodal jet trajectory in flow through scaled models of the human vocal tract," Exp. Fluids **40**, 683–696.

Everstine, G. C. (**2008**). *Applications of Linear Algebra* (The George Washington University, Washington, DC), pp. 64–80.

Fung, Y. C (**1965**), *Foundations of Solid Mechanics* (Prentice-Hall Inc., Englewood Cliffs, NJ), pp. 1–455.

Goodyer, E., Muller, F., Bramer, B. Chauhan, D., Hess, M. (**2006**). "In vivo measurement of the elastic properties of the human vocal fold," Eur. Arch. Otorhinolaryngol. **263**, 445–462.

Goodyer, E. Hemmerich, S. Muller, F. Kobler, J., and Hess, M. (**2007a**). "The shear modulus of the human vocal fold, preliminary results from 20 larynxes," Eur. Arch. Otorhinolaryngol. **264**, 45–50.

Goodyer, E., Muller, F., Licht, A., and Hess, M. (**2007b**). "In vivo measurement of the shear modulus of the human vocal fold—Interim results from 8 patients," Eur. Arch. Otorhinolaryngol. **264**, 631–635.

Goodyer, E., Selham, N. V., Choi, S. H., Yamashita, M., and Dailey, S. H. (**2009**). "The shear modulus of the human vocal fold in a transverse direction," J. Voice **23**(2), 151–155.

Heinrich, R., and Rapoport, T. A. (**1974**), "A linear steady-state theory of enzymatic chains: general properties, control and effector strength," Eur. J. Biochem. **42**, 89–95.

Hirano, M. (**1974**). "Morphological structure of the vocal cord as a vibrator and its variations," Folia Phoniatr. **26**, 89–94.

Hirano, M. (**1977**). "Structure and vibratory behavior of the vocal folds," *Dynamic Aspect of Speech Production* (University of Tokyo Press, Tokyo, Japan), pp. 13–27.

Hirano, M., Kurita, S., and Nakashima, T. (**1981**). "The structure of the vocal folds," *Vocal Fold Physiology*, edited by K. Stevens and M. Hirano (University of Tokyo, Tokyo), pp. 33–41.

Hirano, M. (**1975**). "Phonosurgery: basic and clinical investigations," Official Rep. 76th Annual Convention on Oto-Rhino-Laryngo. Soc., Jurume, Japan.

Jun, B. C., Kim, H. T., Kim, H. S., and Cho, S. H. (**2005**). "Clinical feasibility of the new technique of functional 3D laryngeal CT," Acta Oto Laryngol. **125**, 774–778.

Kacser, H., and Burns, J. A. (**1995**). "The control of flux," Biochem. Soc. Trans. **23**, 341–366.
Kim, B. S., Ahn, K. J., Park, Y. H., and Hahn, S. T. (**2008**). "Usefulness of laryngeal phonation CT in the diagnosis of vocal fold paralysis," Am. J. Roentgenol. **190**, 1376–1379.
Klemuk, S. A., and Titze, I. R. (**2004**). "Viscoelastic properties of three vocal fold injectable biomaterials at low audo frequencies," Laryngoscope **114**, 1597–1603.
Luo, H., Mittal, R., Bielamowize, S., Walsh, R., and Hahn, J. (**2008**). "An immersed-boundary method for flow-structure interaction in biological systems with applications to phonation," J. Comput. Phys. **227**, 9303–9332.
Mihaescu, M., Khosla, S. M., Murugappan, S., and Gutmark, E. J. (**2010**). "Unsteady laryngeal airflow simulations of the intra-glottal vertical structures," J. Acoust. Soc. Am. **127**(1), 435–444.
Min, Y. B., Titze, I. R., and Alipour, F. (**1996**). "Stress-strain response of the human vocal ligament," Annals of Otology, Rhinol. Laryngol. **104**, 563–569.
Moore, P., and Von Leden, H. (**1958**). "Dynamic variations of the vibratory pattern in the normal larynx," Folia Phoniatr. (Basel) **10**(4), 205–238.
Philips, R., Zhang, Y., Keuler, M., Tao, C., and Jiang, J. J. (**2009**). "Measurement of liquid and solid component parameters in canine vocal fold lamina propria," J. Acoust. Soc. Am. **125**(4), 2282–2287.
Rosa, M. D. O., Pereira, J. C., Grellet, M., and Alwan, A. (**2003**). "A contribution to simulating a three-dimensional larynx model using the finite element method," J. Acoust. Soc. Am., **114**(5), 2893–2905.
Scherer, R. C., Shinwari, D., Witt, K. J., Zhang, C., Kucinschi, R., and Afjeh, A. A. (**2001**). "Intraglottal pressure profiles for a symmetric and oblique glottis with a divergence angle of 10 degrees," J. Acoust. Soc. Am. **109**(4), 1616–1630.
Scherer, R. C., Shinwari, D., Witt, K. J., Zhang, C., Kucinschi, R., and Afjeh, A. A. (**2002**). "Intraglottal pressure distributions for a symmetric and oblique glottis with a uniform duct (L)," J. Acoust. Soc. Am. **112**(4), 1253–1256.
Scherer, R. C., Torkaman, S., Kucinschi, B. R., and Afjeh, A. A. (**2010**). "Intraglottal pressure in a three-dimensional with a non-rectangular glottal shape," J. Acoust. Soc. Am. **128**(2), 828–838.
Shinwari, D., Scherer, R. C., Witt, K. J., and Afjeh, A. A. (**2003**). "Flow visualization and pressure distributions in a model of the glottis with a symmetric and oblique divergent angle of 10 degrees," J. Acoust. Soc. Am. **113**(1), 487–497.
Story, B. H., and Titze, I. R. (**1995**). "Voice simulation with a body-cover model of the vocal folds," J. Acoust. Soc. Am. **97**(2), 1249–1259.
Tao, C., and Jiang, J. J. (**2007**). "Mechanical stress during phonation in a self-oscillating finite-element vocal fold model," J. Biomech. **41**, 2191–2198.
Titze, I. R. (**1994**), *Principles of Voice Production* (Prentice-Hall, Englewood Cliffs, NJ), pp. 15–20.
Titze, I. R. (**1988**). "The physics of small-amplitude oscillation of the vocal folds," J. Acoust. Soc. Am.**83**, 1536–1552.
Titze, I. R., Klemuk, S. A., and Gray, S. (**2004**). "Methodology for theological testing of engineered biomaterials at low audio frequencies," J. Acoust. Soc. Am. **115**, 392–401.
Zhang, K., Siegmund, T., and Chan, R. W. (**2006**) "A constitutive model of the human vocal fold cover for fundamental frequency regulation," J. Acoust. Soc. Am. **199**(2), 1050–1062.
Zhang, Z., Neubauer, J., and Berry, D. A. (**2006**). "Aerodynamically and acoustically driven modes of vibration in a physical model of the vocal folds," J. Acoust. Soc. Am. **120**(5), 2841–2849.
Zhang, Z., Neubauer, J., and Berry, D. A. (**2007**). "Physical mechanisms of phonation onset: A linear stability analysis of an aeroelastic continuum model of phonation," J. Acoust. Soc. Am. **122**(4), 2279–2295.
Zhang, Z. (**2008**). "Influence of flow separation location on phonation onset," J. Acoust. Soc. Am. **124**(3), 1689–1694.
Zhang, Z. (**2009**). "Characteristics of phonation onset in a two-layer vocal fold model," J. Acoust. Soc. Am. **125**(2), 1091–1102.
Zhang, Z. (**2010**). "Dependence of phonation threshold pressure and frequency on vocal fold geometry and biomechanics," J. Acoust. Soc. Am. **127**(4), 2554–2562.
Zheng, X., Bielamowicz, S., Luo, H., and Mittal, R. (**2009**). "A computational study of the effect of false vocal folds on glottal flow and vocal folds vibration during phonation," Ann. Biomed. Eng. **37**(3), 625–642.
Zheng, X. (**2009**). "Biomechanical modeling of glottal aerodynamics and vocal fold vibration during phonation," Ph.D. dissertation, George Washington University, Washington, DC, pp. 1–167.